D_N in the individual cases. In consequence the weighting functions for the general case can be simply written down as follows.† Thus, for a centrosymmetric crystal it is given by

$$W_C = \tanh U \tag{10}$$

and for a non-centrosymmetric crystal, by

$$W_A = I_1(2U)/I_0(2U) \tag{11}$$

where

$$U = \sigma_A y_N y_P^c/(1-\sigma_A^2) \tag{12}$$

and

$$\sigma_A = \sigma_1 \langle \cos 2\pi \mathbf{H} \,.\, \Delta \mathbf{r}_j \rangle_P = \sigma_1 D_P \,. \tag{13}$$

It may be verified that when $P=N$, $\sigma_1=1$ so that expressions (10) and (11) reduce to (8) and (9) respectively. On the other hand when the errors are all zero, $D_P=1$ so that $\sigma_A=\sigma_1$ and expressions (10) and (11) reduce to (3) and (4) respectively. Thus, when finite errors exist in the coordinates of the known P atoms the effective value gets reduced from σ_1 to $\sigma_1 D_P$ since D_P is always less than unity.

In order to be able to apply (8) and (11) in practice, a knowledge is required of the parameter σ_A. Methods of obtaining this from the experimental data have been suggested and are discussed in the paper cited above (Srinivasan & Ramachandran, 1965). It involves mainly the evaluation of one or both of two parameters $\langle R_1 \rangle$ and Z^c which have been termed the normalized reliability index and the amplitude correlation respectively and are given by

$$R_1 = \frac{\Sigma ||F_N| - |F_P^c|/\sigma_1|}{\Sigma |F_N|} \tag{14}$$

$$\langle Z^c \rangle = \frac{\Sigma |F_N|\,|F_P^c|}{(\Sigma |F_N|^2\, \Sigma |F_P^c|^2)^{\frac{1}{2}}} \,. \tag{15}$$

† For a formal proof of the results see Srinivasan & Chandrasekharan (1965).

Both R_1 and $\langle Z^c \rangle$ as a function of σ_A are available (Srinivasan & Ramachandran, 1965). It may be pointed out that since σ_A involves D_P it is strongly dependent on the Bragg angle θ, and hence the evaluation of the parameters R_1 and $\langle Z^c \rangle$ has to be done over a narrow region in the reciprocal space within which θ can be assumed to be constant. One could thus obtain σ_A as a function of θ which could then be used in (12).

It may be pointed out, however, that although theoretically the correct weighting functions to be used when the known atoms have errors in their atomic coordinates are given by (10) and (11), from the point of view of practical efficiency it becomes important, before applying these functions, to refine the coordinates of the known P atoms so as to minimize the errors in them. This is obvious from the nature of the functions. The larger the value of σ_A the larger will be the values of W, the maximum value of σ_A for any given σ_1 being σ_1 which would correspond to no errors in the positions of the P atoms. Preliminary refinement of the known atoms would ensure a value of σ_A as close to σ_1 as possible.

References

LUZZATI, V. (1952). *Acta Cryst.* **5**, 802.
MAZUMDAR, S. K. (1964). *Acta Cryst.* **17**, 1082.
QURASHI, M. M. & VAND, V. (1953). *Acta Cryst.* **6**, 341.
SIM, G. A. (1960). *Acta Cryst.* **13**, 511.
SRINIVASAN, R. & CHANDRASEKHARAN, R. (1965). *Indian J. Pure Appl. Phys.* In the press.
SRINIVASAN, R. & RAMACHANDRAN, G. N. (1965). *Acta Cryst.* **19**, 1008.
VAND, V. & PEPINSKY, R. (1957) *Acta Cryst.* **10**, 563.
WOOLFSON, M. M. (1956). *Acta Cryst.* **9**, 804.

Acta Cryst. (1966). **20**, 144

Dispersion of the strain optical ratios in cubic crystals.

By A. RAHMAN and K. S. IYENGAR, *Department of Physics, Osmania University, Hyderabad, A. P., India*

(*Received* 19 *July* 1965)

With the experimental set-up shown in Fig. 1, we have studied the variation of the strain-optical ratios P_{12}/P_{11} and $P_{44}/P_{11}+P_{12}$ for a few cubic crystals in the wavelength range 2500–6000 Å. Light from a 400-watt Hanovia arc after passing through an adjustable horizontal slit S is collimated by the lens L_1. The collimated beam then enters the crystal C under investigation, a double image prism D and finally the quartz prism Q of a medium quartz spectrograph. When the length of the slit is suitably adjusted, the prominent lines of the mercury spectrum are recorded as two sets of horizontal lines, one above the other, on the photographic plate placed at PP (Fig. 1; see also Fig. 2). The crystal rests on the ultrasonic transducer T and when suitably excited a longitudinal standing wave is set up in it. This results in each spectral line being split up into a number of diffraction orders giving rise to the familiar Hiedemann pattern. Mueller (1938; see also Bergmann & Fues, 1936) has shown, on theoretical grounds, that the ratio of the intensities of the corresponding diffraction lines of the mth order in the two polarized sets has the value $B_m^0 = R^{2m}$, where B_m^0 is the limiting ratio of intensities when the sound amplitude is reduced to zero; and $R = P_{12}/P_{11}$ or $P_{11}+P_{12}-2P_{44}/P_{11}+P_{12}+2P_{44}$ depending on the direction of propagation of sound in the crystal along [100] or [110] respectively and the light beam travelling in a direction normal to that of sound along a cube axis.

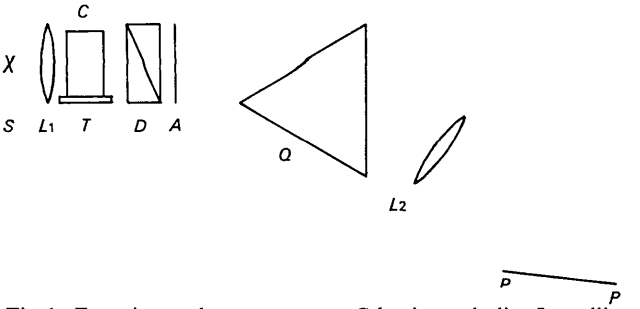

Fig. 1. Experimental arrangement. S horizontal slit, L_1 collimator lens, C crystal specimen, T transducer, D double image prism, A analyser, Q quartz prism, L_2 camera lens, PP photographic plate.

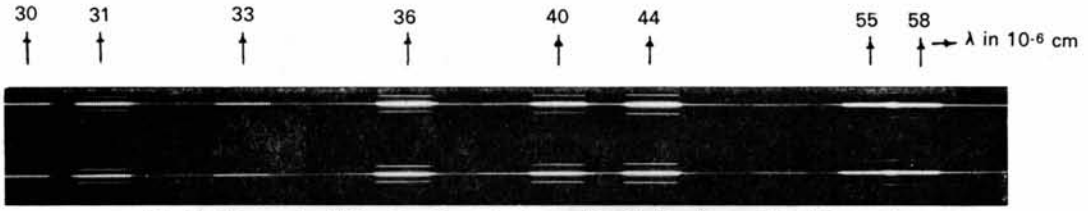

Fig. 2. Ultrasonic diffraction in potassium chloride for lines of the Hg spectrum.

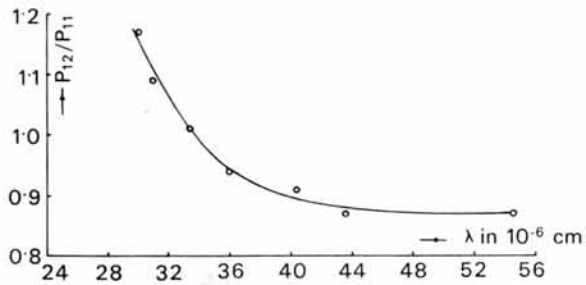

Fig. 3. Strain-optical dispersion of potassium iodide.

At low levels of ultrasonic excitation only the first diffraction order is recorded and the relative intensity of the corresponding two spectral sets is determined with the help of an analyser (Polaroid sheet HNP'B) interposed at A (Fig. 1) following the double image prism D. B_m is obtained from the identity, $B_m = \tan^2 \alpha$, where α is the angle through which the analyser is rotated in order to equalize the intensities of the corresponding spectral images. In practice this was realized by photographing the pattern for various positions of the analyser at 2° intervals and measuring the relative intensities with a microphotometer. The position of equal intensities was then determined by interpolation. This process was repeated for a few values of sound amplitude in decreasing order and the limiting ratio B_m^0 was then obtained. In Fig. 3 the variation of the ratio P_{12}/P_{11} with wavelength of light is shown for potassium iodide. Similar curves have been obtained for potassium bromide and potassium chloride. The ratio attains the value unity at a wavelength characteristic of the solid. For light of this wavelength the solid fails to exhibit birefrigence under stress, when the stress is applied in the direction of the cube axis and observation is made along a different axis. The characteristic wavelengths obtained in this manner are in good agreement with those reported by Srinivasan (1959) who studied the variation of the difference $(P_{11} - P_{12})$ by a static method. In Fig. 4(*a*) the dispersion of the ratios $P_{44}/P_{11} + P_{12}$, P_{44}/P_{11} and P_{44}/P_{12} for sodium chloride has been shown. The dispersion graphs for potassium bromide, potassium iodide, and sodium chloride are very similar.

With differences $(P_{11} - P_{12})$ determined by Srinivasan and the ratios obtained by us, the absolute values of the strain-optical constants have been determined. These are shown for NaCl in Fig. 4(*b*). In the short wave region of the spectrum P_{11} undergoes much larger changes than P_{12}. This

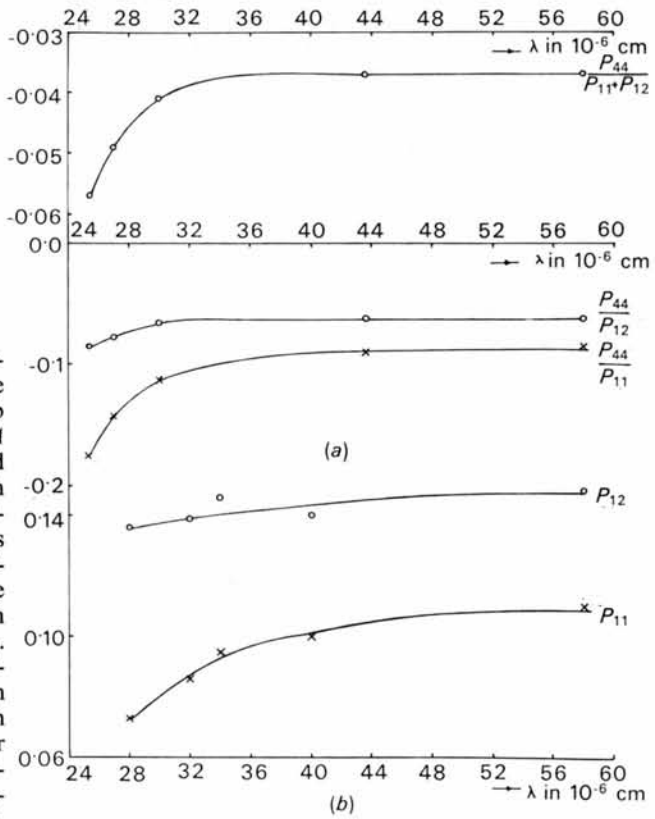

Fig. 4. Strain-optical dispersion of sodium chloride. (*a*) Ratios P_{44}/P_{11}, $+P_{12}$, P_{44}/P_{11}, P_{44}/P_{12}. (*b*) Values of P_{11} and P_{12}.

feature is common to other alkali halides and accounts for the larger variation of P_{44}/P_{11} when compared with P_{44}/P_{12}, since the dispersion of P_{44} is small (Bansigir & Iyengar, 1961).

References

BANSIGIR, K. G. & IYENGAR, K. S. (1961). *Acta Cryst.* **14**, 727.

BERGMANN, L. & FUES, E. (1936). *Naturwissenschaften,* **24**, 492.

MUELLER, H. (1938). *Z. Kristallogr.* A, **99**, 122.

SRINIVASAN, R. (1959). *Z. Phys.* **155**, 281.